'96-5·2

FLUIDIC PRESSURE PULSE TRANSMITTING FLOWMETERS FOR REMOTE OIL FLOW MEASUREMENT

H Wang, G H Priestman, S B M Beck and R F Boucher*

Department of Chemical and Process Engineering, University of Sheffield

*Present address: Principal and Vice-Chancellor, UMIST, Manchester

Summary

Details are given of the development of no-moving-part fluidic devices for the measurement of oil flow deep in the production string where the flow is single-phase. Two devices have been investigated which generate pressure pulses at a frequency proportional to the flowrate. The pulses are transmitted via the flowing two-phase mixture for detection downstream. A balance has been struck between pulse amplitude and pressure loss in the device so as to minimise any reduction of flow. One of the devices, the Blown Venturi flowmeter, is constructed from an oscillating Coanda Switch attached to a Variable Recovery Venturi. The other one is a Coanda Switched Vortex flowmeter, which is a hybrid device consisting of a Vortex Amplifier and an oscillating Coanda Switch. Optimisation of both flowmetering devices have been conducted and they show good performance over a wide operating range in the laboratory.

1. INTRODUCTION

In oil production, it is important to know how much oil is being supplied from each of the wells, for calculating royalty and working-interest payment, guiding daily production operation, and managing the reservoir. The bottom of these wells are usually several kilometres underground, and tend to be manifolded together to a surface station. As the crude oil approaches the surface, its pressure drops and the gas, which is kept in solution by high static pressure, comes out in bubbles. This can happen to such an extent that what is delivered to the surface is a foam. Conventional measuring devices are not suited to this situation, though some attempts have been made at two-phase flowmetering. Liu et al [1] and Millington et al [2] made this measurement with a separation method, and Baker and Hayes [3] and Fisher [4] tried to develop a metering system for the total mass flow of the multiphase medium.

An alternative approach is to measure the flow rate at the bottom of the well where the flow is still single-phase, though any such device must have high reliability and not reduce production rate. This paper describes development of such a meter which produces pressure pulses at the bottom of the well using a reliable no-moving-part fluidic device, with the frequency proportional to fluid flowrate. The pulses are transmitted through the fluid in the pipe to the surface, where they can be detected and recorded. To minimise any production loss, the mean pressure drop across the device must be kept small.

Pulse transmission of information is well established in oil drilling, where drilling mud is the fluid medium [5]. Measurement-while-drilling (MWD) techniques generate pulses, sent through the drilling mud to the drilling platform [6], and successful pulse reception after transmission over more than a kilometre is proven for single phase media. In oil production, the additional complication of two phase flow is present, with much greater attenuation beyond the bubble point. Experiments and computer modelling are therefore being conducted to determine suitable pulse amplitudes. Some compensation can be obtained, if needed, by locating the pulse detector on the sea bed rather that at the well-head.

Many studies have been done on the development of fluid oscillatory type flowmeters, which can be classified [7] as, fluidic oscillator, vortex-precession swirlmeter [8, 9] and vortex shedding flowmeter [10]. Fluidic oscillators, which include relaxation and feedback oscillators [11] work on the principle of the Coanda effect. The frequency of oscillation of the jet is a measurement of the flowrate. Although much work has been done on this type of flowmeter [12, 13, 14, 15, 16], none of the meters combine sufficient pressure pulse amplitude with the low overall pressure loss required in the proposed application.

Two fluidic flowmeter devices have been developed in this study. One, the Blown Venturi (BV) flowmeter, is constructed from an oscillating Coanda Switch attached to a Variable Recovery Venturi (VRV). The other one is a Coanda Switched Vortex (CSV) flowmeter, which is a hybrid device consisting of a Vortex Amplifier and an oscillating Coanda Switch. For both devices experiments have been conducted to optimise their geometry with respect to minimising total pressure drop, maximising pulse amplitude and ensuring a satisfactory relationship between pulse frequency and flowrate. Comparative data for the two devices should enable their relative merits to be assessed for use as oil flow measuring devices.

The downhole flowmeter produces pressure pulses which are transmitted by wave action to the well head. The analysis of the pulse transmission to ascertain if there is still sufficient signal at the surface to measure is clearly important. Because of the difficulty of experimentally modelling pressure pulse transmission in a vertical flow of crude oil-natural gas mixture, a computer programme called SUNAS [17] with Transmission Line Modelling [18] is being used to model pressure pulse transmission attenuation in vertical air-water bubble flow. The prediction can then be compared with experimental measurements being done with an air-water pipe rig . The air-water model can be adapted for vertical oil two-phase flow by use of a suitable attenuation coefficient. CFD modelling [19] using a time dependant boundary is also going to be used for modelling the air/water and oil/gas bubbly flow for comparison with both the predicted attenuation and the experimental measurements. This will be reported [20] in due course.

2. BLOWN VENTURI (BV) FLOWMETER

The Blown Venturi flowmeter (Fig.1) is constructed from an oscillating Coanda Switch attached to a Variable Recovery Venturi. The flow through the oscillating Coanda Switch acts as a small by-pass flow past the venturi. When there is no flow in control pipe "1", connected to the venturi throat, the overall pressure loss of the device, ΔP, is very low. When flow is introduced from control pipe "1" to the throat, it upsets the boundary layer and reduces the pressure recovery, increasing the pressure drop across the device. Introducing flow through control pipe "2" has little effect on ΔP. Using a control loop to connect together the control ports of the Coanda Switch causes the jet in the switch to alternate between control pipe 1 and 2 and so causes the VRV pressure drop to switch between a high and a low value. The device works as a flowmeter because the frequency of the oscillating Coanda switch is proportional to the flowrate going through it, so by measuring the frequency of the oscillations downstream, the flowrate can be measured.

Tests with low pressure air have been carried out [21] to optimise the design. Optimum performance was found to correspond to the following design:

- divergence angle, $\theta = 16°$;
- venturi area ratio AR (outlet area/throat area) = *7.0;*
- size ratio (venturi inlet area/Coanda supply nozzle area) = *122.*

Based on these findings a brass device was designed for operation with water. Experimental work was done to study the effect of control loop geometry on the oscillation frequency, overall pressure drop and pulse amplitude.

Fig.2 shows the profile of the brass flowmeter. This device was constructed out of two pieces (body and lid) of brass. To measure the static performance a test arrangement was set up as shown in Fig.3. The outlet jet of the Coanda device was alternatively switched by introducing a control flow Q_{cL} or Q_{cH}, whilst the device outlet flow, Q_e, was held at a constant value. For example, to measure the low resistance state, valves H and L were closed, then valve L was briefly opened. In this way the jet from the Coanda supply nozzle was discharged through the control pipe "2" (Fig.1), the

jet remaining in this low resistance state due to the Coanda effect. Briefly opening valve H induced switching to the high resistance state. Measuring the pressure drop ($\Delta P = P_s - P_a$) of this device, at high and low resistance states, with different exit flows, allowed ΔP_{high} and ΔP_{low} to be measured.

For measuring static performance an important quantity is the Turndown Ratio N, given as

$$N = \sqrt{\frac{Eu_{high}}{Eu_{low}}} \tag{1}$$

where

$$Eu_{high} = \frac{\Delta P_{high}}{0.5\rho V_0^2}, \quad \text{and} \quad Eu_{low} = \frac{\Delta P_{low}}{0.5\rho V_0^2} \tag{2}$$

For constant flow, this turndown ratio simplifies to:

$$N = \sqrt{\frac{\Delta P_{high}}{\Delta P_{low}}} \tag{3}$$

where Eu is the Euler number for each resistance state, ρ is the fluid density, V_0 is the average fluid velocity based on the flow in the outlet pipe for the meter. Since the flowmeter should constitute only a small part of whole system resistance, the condition maintained during switching should approximate to one of constant flow. Hence, with constant pressure upstream of the flowmeter, N gives an indication of the strength of the pressure pulse downstream of the device. Fig.4 shows the variation of turndown ratio with Reynolds number again based on the venturi outlet pipe. It can be seen that increasing flowrate gives an increase in turndown ratio, so the flowmeter operation is more effective at higher flowrates, although N does tend toward a constant value.

To obtain the operating performance of this flowmeter, a control loop was connected between the Coanda switch control ports to create an oscillating Coanda system. This control loop can be modelled as a fluid transmission line with zero mean flow and laminar oscillating flow. Tippetts et al [22] studied this oscillating Coanda switch as a flowmeter, and deduced a dimensionless control loop inductance as:

$$L' = 4l' n / (\pi d'^2) \tag{4}$$

where:

$$l' = l / d_n \quad \text{and} \quad d' = d / d_n \tag{5}$$

l and d are the length and diameter of the control loop, and n and d_n the aspect ratio and width of the Coanda supply nozzle respectively. L' is a factor required to be held the same if frequencies are to scale with size changes. Essentially it measures the ratio of the inductance of the pipe to that of the Coanda switch body.

Fig.5 shows the rig used to detect the pressure pulses generated by this device. The dynamic differential pressure pulses were captured by means of a differential pressure transducer (Druck®, PDCR 190-1436, ±1 bar). The differential pressure pulse wave forms (Fig.6) were directly monitored by an oscilloscope and an electronic signal analyzer connected to the transducer. A personal computer equipped with a data acquisition board was also used to capture the differential pressure pulse signals from the transducer. 'GLOBAL LAB®' software was used, with a sample rate of *2000* Hz. For the meter operating with a control loop inductance, $L'=141$, differential pressure pulses are shown in Fig.6 for several flowrates. Pulse amplitude A (defined as ΔP_{max} - ΔP_{min} from the oscillation data) and mean pressure drop ΔP, are important parameters for the flowmeter operating performance. Fig.6 shows an increase in both the pulse amplitude and frequency, f, with increasing flowrate. The important operational parameters, however, are frequency per unit volume f/Q and relative pulse amplitude A' $(=A/\Delta P)$. Both of these criteria are found to be affected by the dimensions of the control loop. Fig.7 shows how f varied with Q for different control loop dimensions. For any fixed value L', f is seen to increase linearly with Q. Increasing L' is seen to decrease f for a given flowrate. It can be seen from Fig.7 that Q increasing from *0.00027* to *0.00102* m^3/s corresponds to an oscillation frequency f, increasing from about *2.0* to *12.0* Hz for $L'=141$. The flowrate vs. frequency relationship is seen to be linear. A linear regression was applied to the data to give a fitted curve,

$$Q\ (m^3/s) = 7.41 \times 10^{-5} f\ (Hz) + 1.53 \times 10^{-4} \tag{6}$$

Thus the linear relationship between f and Q does not pass through the origin and the rate f/Q is not constant, although it tends toward a single value at high frequencies, when the intercept become less significant.

Fig.8 shows the effects of L' on the relative pulse amplitude A', over the tested flow range. The largest pulses, relative to overall pressure drop, are seen to corresponds to $L' = 141$, which corresponded to $l = 0.6$ m and $d = 5$ mm in the device tested. Fig.9 shows the variation in meter pressure drop with flowrate, both for oscillation operation, and standby mode. Standby occurs with the control loop blocked so the device acts as a low resistance venturi. Thus having a means of blocking the control loop enables the meter to be de-activated, with an associated saving in pressure loss.

3. COANDA SWITCHED VORTEX (CSV) FLOWMETER

A Vortex Amplifier (VA) is attached to an oscillating Coanda switch to create a Coanda Switched Vortex (CSV) flowmeter (Fig.10). This device has two flow states, of high and low resistance respectively. The Coanda switch must be suitably matched to the VA such that one Coanda switch leg feeds all the flow to the VA tangential port, producing a vortex and leading to high resistance. The radially directed flow from the other Coanda outlet gives the low resistance mode (Fig.10). If an oscillating Coanda switch is employed, the flowmeter inlet flow will be alternatively switched to the two VA inlets, resulting in the production of a large pressure pulse.

The Coanda Switched Vortex was first introduced by Adams and Moor [23], and also studied by Tippetts [24]. The closest application of the Coanda Switched Vortex to that envisaged for remote flow measurement was the fluidic hydraulic ram [25] and the fluidic hammer for percussion drilling [18]. Both of these devices are, however, unsuited to flow measurement because of their high overall mean resistance and the significant flow interruptions, which would generally be unacceptable in an oil production string.

Fig.11 shows a traditional shape of VA. The flow through the radial port experiences a low resistance, since the flow has only to pass through a successive

sudden expansion into the VA chamber and the contraction at the exit of the device. The high resistance state occurs when the flow enters the tangential inlet port. The flow swirls inside the VA chamber producing a strong vortex exit flow which greatly increases the energy losses of the system through turbulent eddies. The effect of geometry on VA operation has been studied widely in the past [26, 27, 28, etc.]. Unfortunately, the traditional VAs such as in Fig.11 cannot easily be connected in series with a Coanda switch and positioned downhole inside an oil producer, because the two inlet connection pipes extend beyond the boundaries of the circular VA chamber. A new kind of 'in-line' VA (Fig.12) was needed to better fit the drill string. This VA is designed to have inlet ports opposite the exit port, such that all the pipes are parallel to the pipe housing. This requires that the flow turns through a *90°* angle on entering the chamber. The in-line VA has a thin vortex chamber to achieve a high resistance and a total divergence *6°* exit diffuser to help pressure recovery in the low resistance state. The inlet ports are directed by an internal guide, with high resistance flow directed around the periphery of the chamber.

Due to the geometrical restriction of the industry-standard producer pipe, the VA chamber had to be *125* mm (*5* inches) diameter for the present study. To arrive at the optimum in-line VA size, some theoretical and experimental work was done [29] for matching the Coanda switch to the in-line VA. The best area ratio of the VA exit to the and Coanda switch supply nozzle was determined as *0.8*, this giving a Coanda flowmeter maximum turndown ratio of *1.49*. The exit diameter of the in-line VA was *24* mm and the VA inlet ports diameters were both *33* mm.

An experimental rig similar to Fig.5 was used to measure the meter performance with air. Different control loop designs (diameter from *20* to *40* mm, and length from *0.7* to *2.7* m) were used. Fig.13 shows the flowmeter calibration for different values of the dimensionless control loop inductance L'. It can be seen that flowrates from *0.004* to *0.024* m^3/s corresponded to oscillation frequencies from *0.48* to *5.13* Hz for $L' =$ *206*. As with the venturi meter, the flowrate vs. frequency relationship was linear but did not pass through the origin, the fitted curve being:

$$Q\ (m^3/s) = 4.39\times10^{-3} f\ (Hz) + 1.84\times10^{-3} \qquad (7)$$

Fig.13 also shows that the number of cycles per unit volume *(f/Q)* for $L' = 206$ again tends to a single value at high flows. Fig.14 shows that the relative pulse amplitude *(A/ΔP)* changes with L' over the range of flowrates. $L'=206$ is seen to give best performance, corresponding to a control loop length of *2.5* m and diameter of *25* mm. Again, as with the venturi meter, blocking the control loop put the meter into a low pressure drop standby mode, as shown in Fig.15.

4. SELECTION OF FLOWMETERS FOR OIL FLOW MEASUREMENT

The choice between the venturi and CSV type meters for downhole oil flow measurement depends on the measurement requirements, flowmeter characteristics and flowmeter construction. The relative pressure pulse amplitudes generated are compared in Fig.16 for a range of *Re*, in each case for optimum L'. The Reynolds numbers, in each case is based on flow in the outlet pipe:

$$Re = \frac{V_o d_o}{\nu} \tag{8}$$

where d_o is the flowmeter outlet diameter and the average outlet flowmeter velocity $V_o = Q/A_o$, where Q is the volume flowrate and A_o the outlet cross sectional area, ν is the fluid kinematic viscosity. It is can be seen that the Coanda's relative pulse amplitude is greater than that for the venturi, particularly at lower Reynolds numbers. Thus for a given operating pressure drop, the Coanda meter would produces larger amplitude pulses.

In order to compare with performance of the venturi and Coanda flowmeters for a given application, the experimental data must be plotted in a dimensionless form, with the pipe flow specified as the reference velocity. The meters can be characterised by the relationship between Reynolds number *Re* (Eqn.8) and non-dimensional group representing frequency and pressure drop:

Strouhal number $$Str = \frac{f d_o}{V_o} \tag{9}$$

Euler number $$Eu = \frac{\Delta P}{0.5\rho V_o^2} \quad (10)$$

where f is the frequency of oscillation, V_o is the average outlet velocity, ΔP is the average pressure drop across the flowmeter and d_o is the outlet pipe diameter.

Fig.17 compares the characteristics for the two meter types. In all cases operation is more effective at the higher Reynolds numbers tested, the Strouhal numbers tending to a constant value and the Euler numbers reaching a minimum value. The venturi meter is seen to have a larger Eu, and so ΔP would be significantly lower than with the CSV. The venturi is seen to given a higher frequency signal than the CSV. The differences can be quantified with reference to a typical application.

Considering a *1000* m long oil production string of diameter *5.0* inches (*0.125* m), volume oil flowrate *20,000* bbl/day (*0.0368* m^3/s), giving an average oil velocity in the producer of *3.0* m/s. At a saturated and gas freed oil bottom hole, the pressure is *200* bar, temperature is *200* °F, oil kinematic viscosity is 1×10^{-5} m^2/s and oil density *757* kg/m^3. The two flowmeters can be scaled from Fig.16 & 17 to give the performance as shown in Table 1.

Table 1 Using flowmeter in an oil production string

flowmeter	*Re no.*	*Str no.*	*Eu no.*	*f* (Hz)	*A*/*ΔP*	*ΔP* (bar)	*A* (bar)	ΔP_f* (bar)	ΔP_r[♆]
Venturi	*37500*	*0.098*	*18*	*2.35*	*0.64*	*0.61*	*0.39*	*42.64*	*1.41*
Coanda	*37500*	*0.02*	*36*	*0.48*	*0.93*	*1.23*	*1.14*	*42.64*	*2.79*

* means frictional pressure loss along the producer pipe

[♆] means % pressure loss in the whole length of producer $\{= \Delta P/(\Delta P + \Delta P_f) \times 100)\}$

As expected the blown venturi gives higher frequencies and lower pressure drop, although in both cases the pressure loss is small compared to the pipe frictional loss. Signal transmission is also important and although Table 1 indicates that a venturi can be fitted into the pipe with lower pressure drop, the pulse amplitude will also be less. If the venturi was reduced in size so as to give the same pulse amplitude as the Coanda, the

ventuti pressure drop would increase to *1.78* bar. Clearly the transmission of the pressure pulse through the pipe fluid is also important and is under consideration [20].

5. CONCLUSIONS

Two types of fluidic oscillatory flowmeter, the blown venturi and the Coanda switched valve, have been developed for downhole oil flowrate measurement. Design data and operating characteristics have been presented for each devices. Pulse amplitude is expressed as a ratio relative to the average operating pressure drop, and pulse frequency increases linearly with the volumetric flowrate. The oscillator control loop inductance is shown to influence meter performance, with an optimum factor found for each device.

The use of non-dimensional groups to represent the characteristics enables the meter performance to be compared in a typical application. The blown venturi meter produces a higher pulse frequency and larger pressure drop, but the pulse amplitude is also lower, compared to the Coanda switched vortex meter.

References:

1 LIU K T, CANFIELD D R and CONLEY J T, application of a mass flowmeter for allocation measurement of crude oil production, SPE Production Engineering, November, 1988.

2 MILLINGTON B C and NEL EXECUTIVE AGENCY, a review of the uncertainties associated with the on-line measurement of oil/water/gas multiphase flow, 6th International Conference on Multi Phase Production, Cannes, France, pp.349-360, BHRA Group Conference Series Publication No.4, June, 1993.

3 BAKER R C and HAYES E R, multiphase measurement problems and techniques for crude oil production systems, Petroleum Review, pp.18-22, November, 1985.

4 FISHER C, development of a metering system for total mass flow and compositional measurements of multiphase/multicomponent flows such as oil/water/air mixtures, Flow Measurement Instrumentation, Vol.5, No.1, pp.31-42, 1994.

5 GEARTHART M, ZIEMER K A and KNIGHT O M, mud pulse MWD systems report, SPE (Society of Petroleum Engineers) paper no.10053, Richardson, Texas, 1983.

6 INGLIS T A, directional drilling, petroleum engineering and development studies, Vol.2, Graham & Trotman, London, 1987.

7 BOUCHER R F, a fluidic flowmeter for industrial and clinical applications, 4th Int. Fluidics Conf., paper B-12, pp.1-24, Varna, Bulgaria, 1972.

8 FURNESS R A, fluid flow measurement, Longman, London, 1989.

9 HAYWARD A T J, flowmeters, a basic guide and source-book for users, MacMillan, 1979.

10 YAMASAKI D, TAKAHASHI A and HONDA S, a new fluidic oscillator for flow measurement, proceedings of 2nd int. symposium on fluid control, measurement, mechanics and flow visualization (FLUCOME '88), Sheffield, 1988.

11 BOUCHER R F and TIPPETTS J R, an investigation into the advantages of fluidics in fluid processing - Part 2, Aero. Res. Inst., Sweden, FFA TN., 1982.

12 TIPPETTS J R, GOLDER J A and GRANT J A, improvements in fluid flow measurement, British Patent no. 1297154, Published 22 Nov. 1972

13 GRANT J and TIPPETTS J R, improvements in or relating fluid flow meters, British Patent no. 1363762, Published 14 Aug. 1974

14 GRANT J and COX A J, improvement in or relating to flowmeters', British Patent no.1453587, 1976.

15 MAZHAROGLU C, low Reynolds number fluidic flowmetering, PhD Thesis, Sheffield University, 1988.

16 BOUCHER R F, MAZHAROGLU C, CHURCHILL D and PARKINSON G J, a fluidic by-pass venturimeter, proceedings of 3rd triennial int. symposium on fluid control, measurement, and visualization (FLUCOME '91), San Francisco, USA, 1991.

17 BECK, S B and BOUCHER R F, Sheffield university network analysis software (SUNAS), Dept. of Mech & Proc. Eng., University of Sheffield, 1993.

18 BECK S M, HAIDER H and BOUCHER R F, transmission line modelling of simulated drill strings undergoing water-hammer, Journal of Mechanical Engineering Science, Proceedings of the Institution of Mechanical Engineers, Vol.209, No. C6, pp.419-427, 1995.

19 FLUENT INC., fluent user's guide, Version 4.3, January, 1995.

20 WANG H, BECK S B M, PRIESTMAN G H and BOUCHER R F, simulation of pressure wave attenuation in a crude oil-natural gas mixture during crude oil extraction (in preparation).

21 BOUCHER R F, BECK S B M and WANG H, a fluidic flowmetering device for remote measurement, Journal of Process Mechanical Engineering, Proceedings of the Institution of Mechanical Engineers, Vol.210, No.E2, pp.93-100, 1996

22 TIPPETTS J R, NG H K and ROYLE J K, an oscillating bistable fluid amplifier for use as a flowmeter, Journal of Fluid Control (Fluidics Quarterly), No.1, Vol.5, January, 1973.

23 ADAMS R B and MOORE C B, flow control apparatus, US patent no. 3267946, 23rd August, 1966.

24 TIPPETTS J R, the characteristics and uses of unvented bistable fluid amplifiers, PhD Thesis, Dept. of Mechanical Engineering, Sheffield University, Sept., 1969.

25 TIPPETTS J R, , the fluidic hydraulic ram and a conjectured pressure amplifier, Fluidics Quarterly, Vol.6, Issue 2, pp.45-53, April, 1974.

26 LAWLEY T J and PRICE D C, design of vortex fluid amplifiers with asymmetrical flow fields, Trans. ASME, Journal of Dynamic Systems, Measurement and Control, Vol.94, pp.82-84, 1972.

27 KING C F, some studies of vortex devices - vortex amplifier performance and behaviour, PhD Thesis, Dept. of Mechanical Engineering and Energy Studies, University College, Cardiff, UK, 1978.

28 BECK S B M, DELIGIANNIS P and BOUCHER R F, a study of the geometrical effects of a vortex amplifier chamber on its performance, proceedings of 4th Triennial Int. Symposium on Fluid Control, Fluid mechanics, and Visualisation (FLUCOME '94), pp.29-34, Toulouse, FRANCE, 1994

29 WANG H, BECK S B M, PRIESTMAN G H and BOUCHER R F, a Coanda switched vortex flowmeter (in preparation).

Figures:

Fig.1. Blown Venturi (BV) flowmeter

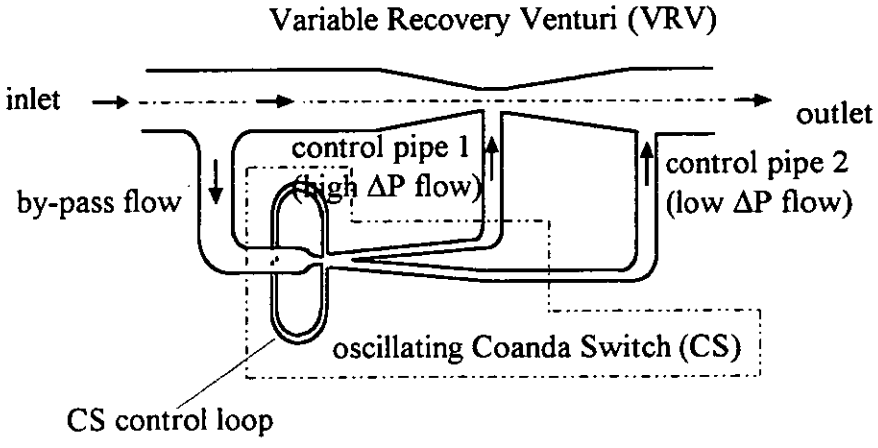

Fig.2. Profile of brass BV flowmeter

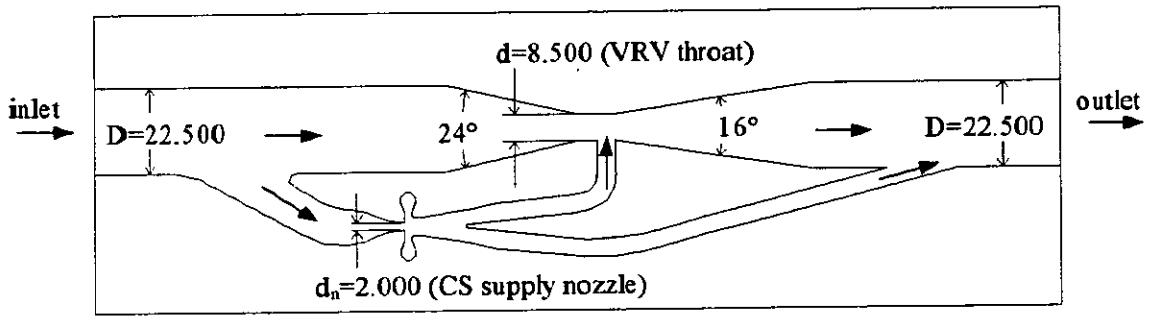

Fig.3. Measure static performance of BV flowmeter for water

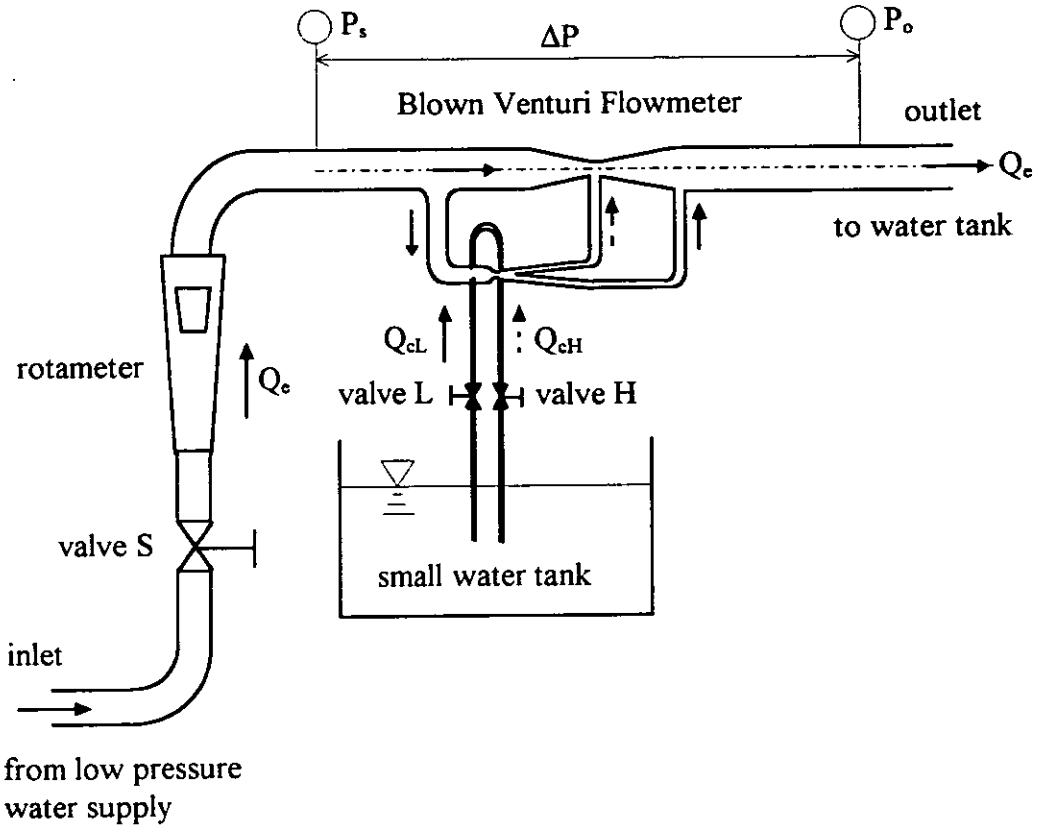

Fig.4. Turndown ratio of BV flowmeter for water test

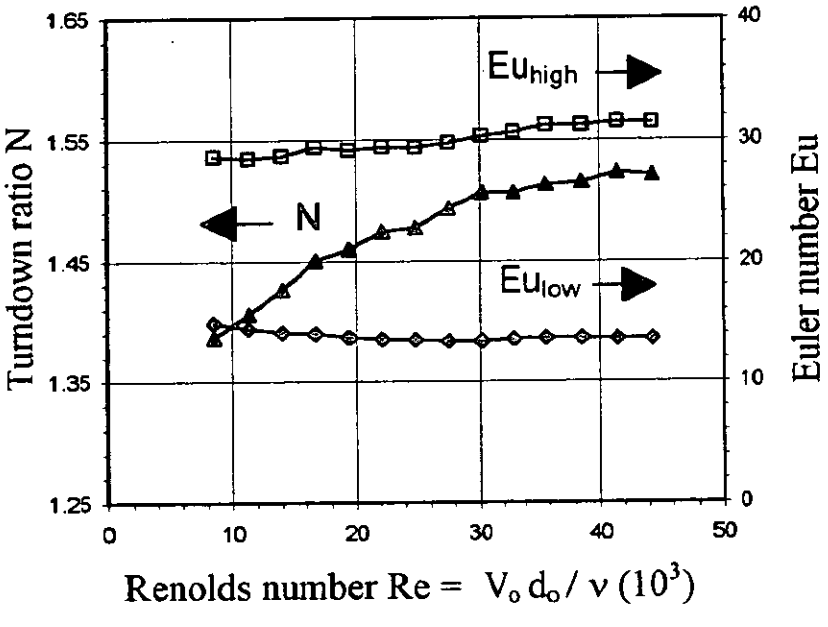

Fig.5. BV flowmeter water test

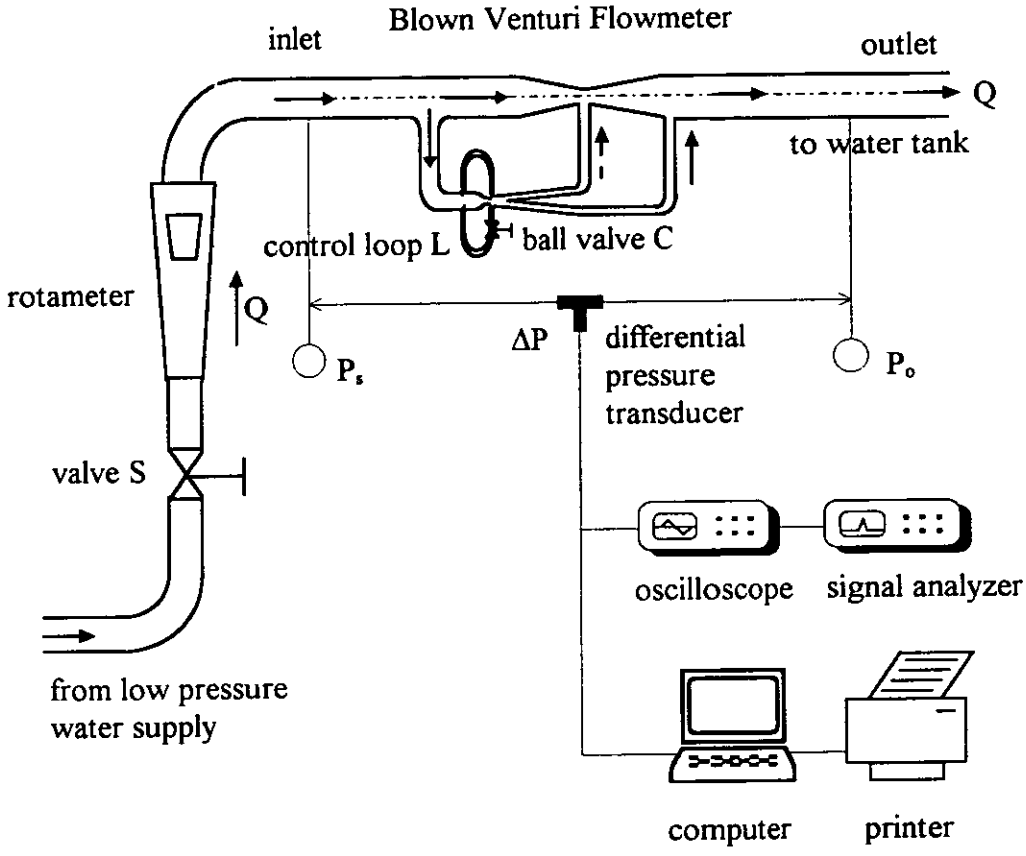

Fig.6. Pressure pulse waveforms

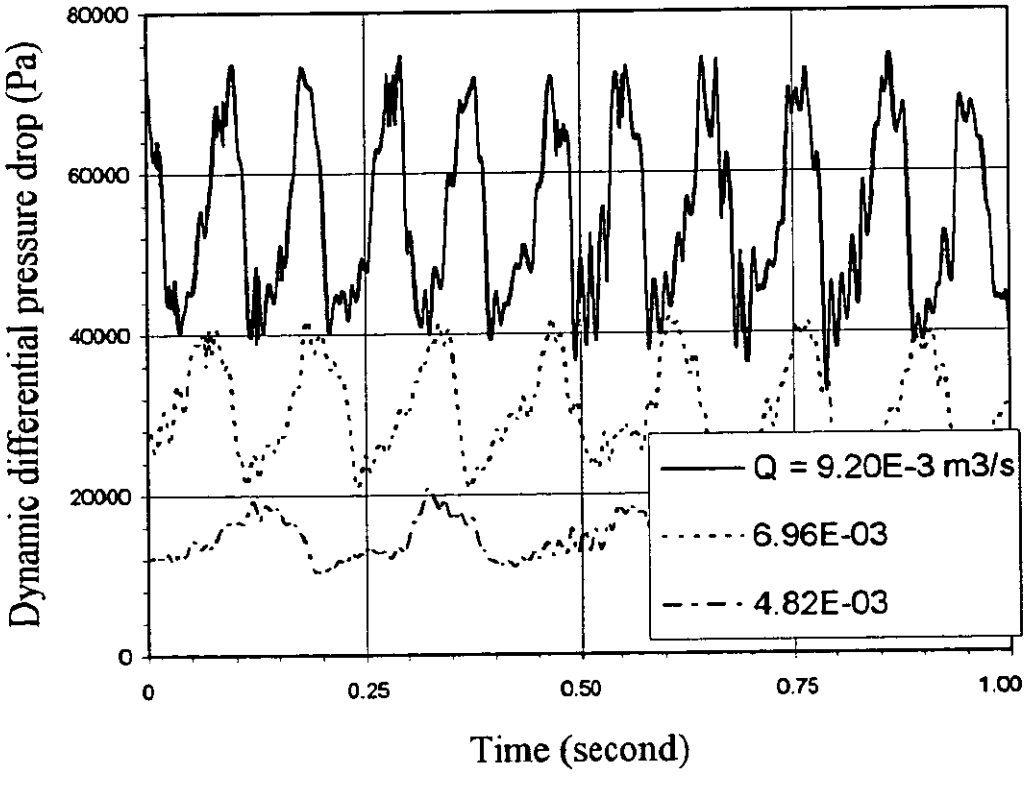

Fig.7. BV flowmeter calibration with dimensionless control loop inductance (L')

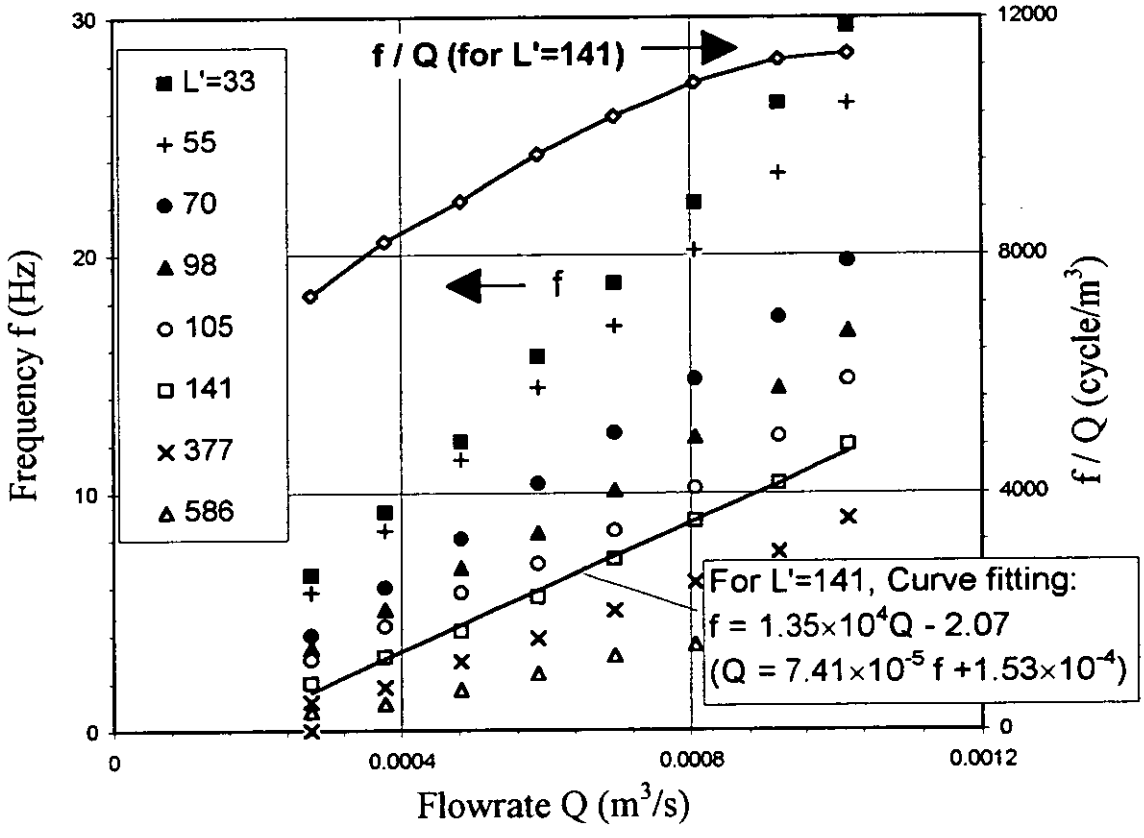

Fig.8. BV flowmeter optimising L' for relative pulse amplitude

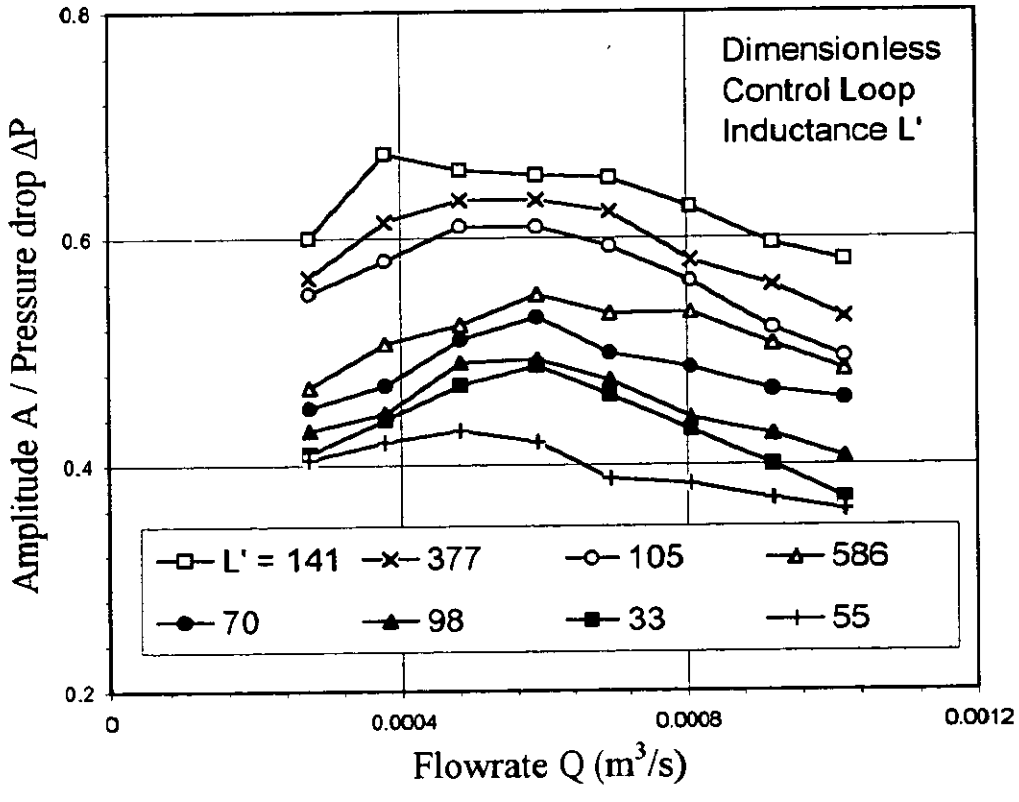

Fig.9. Mean pressure drop of BV flowmeter

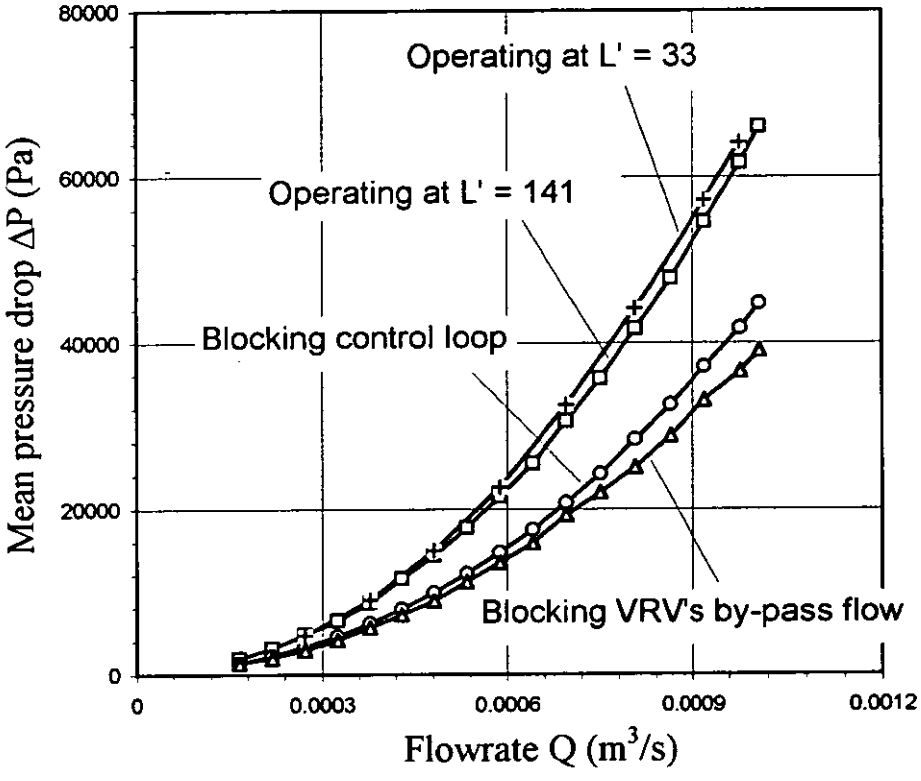

Fig. 10. Coanda Switched Vortex (CSV) flowmeter

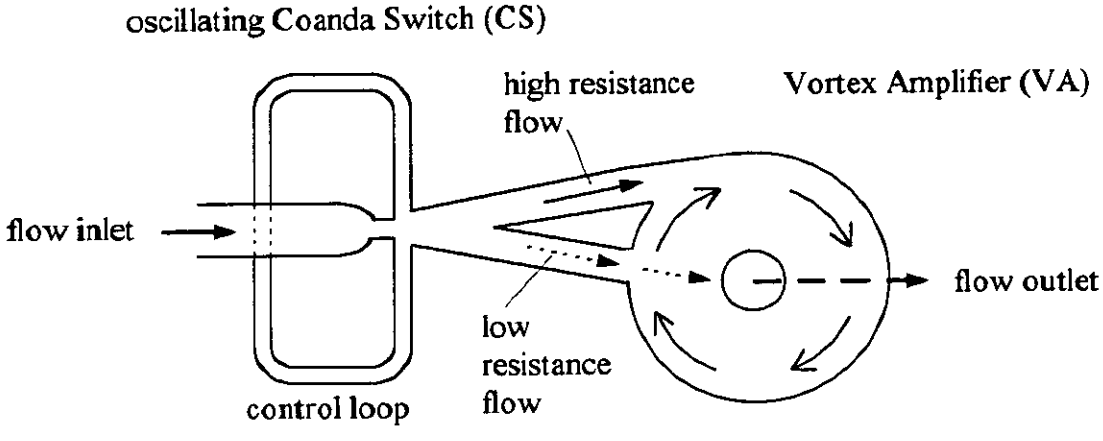

Fig.11. Traditional shape of Vortex Amplifier (VA)

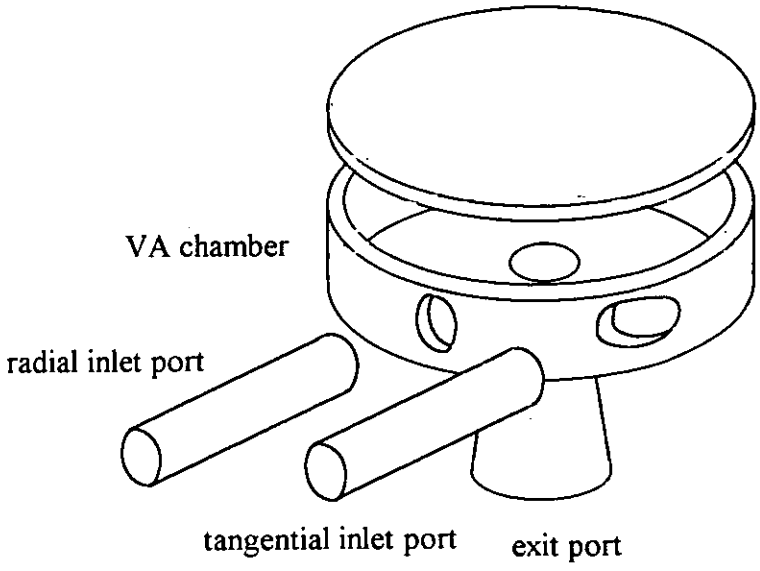

Fig.12. Off-centred port in-line VA

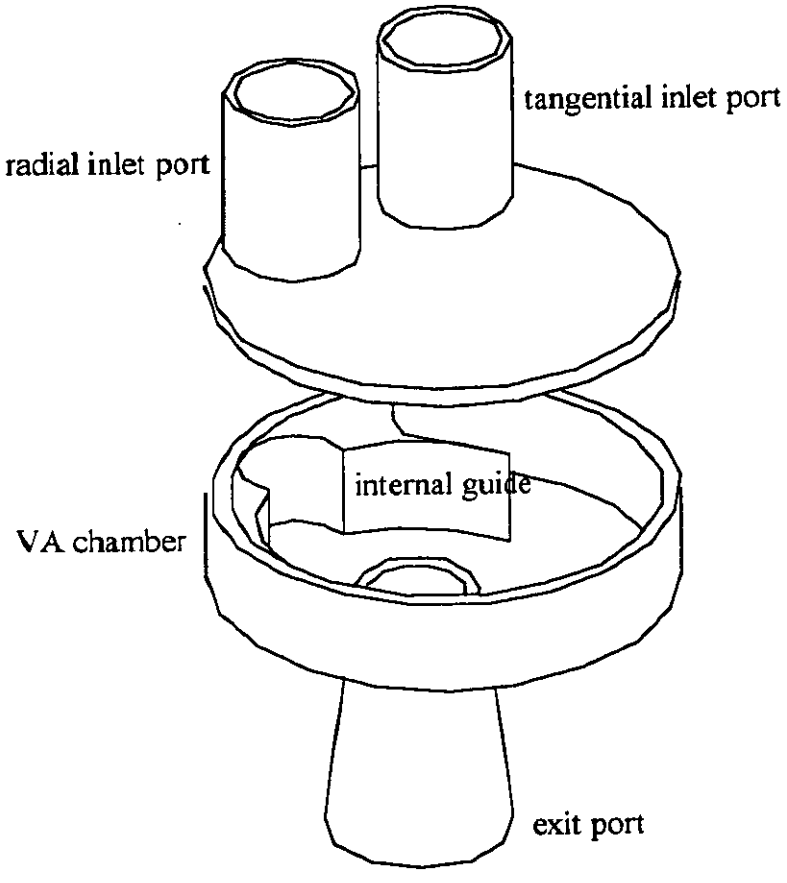

Fig.13. CSV flowmeter calibration with dimensionless control loop inductance (L')

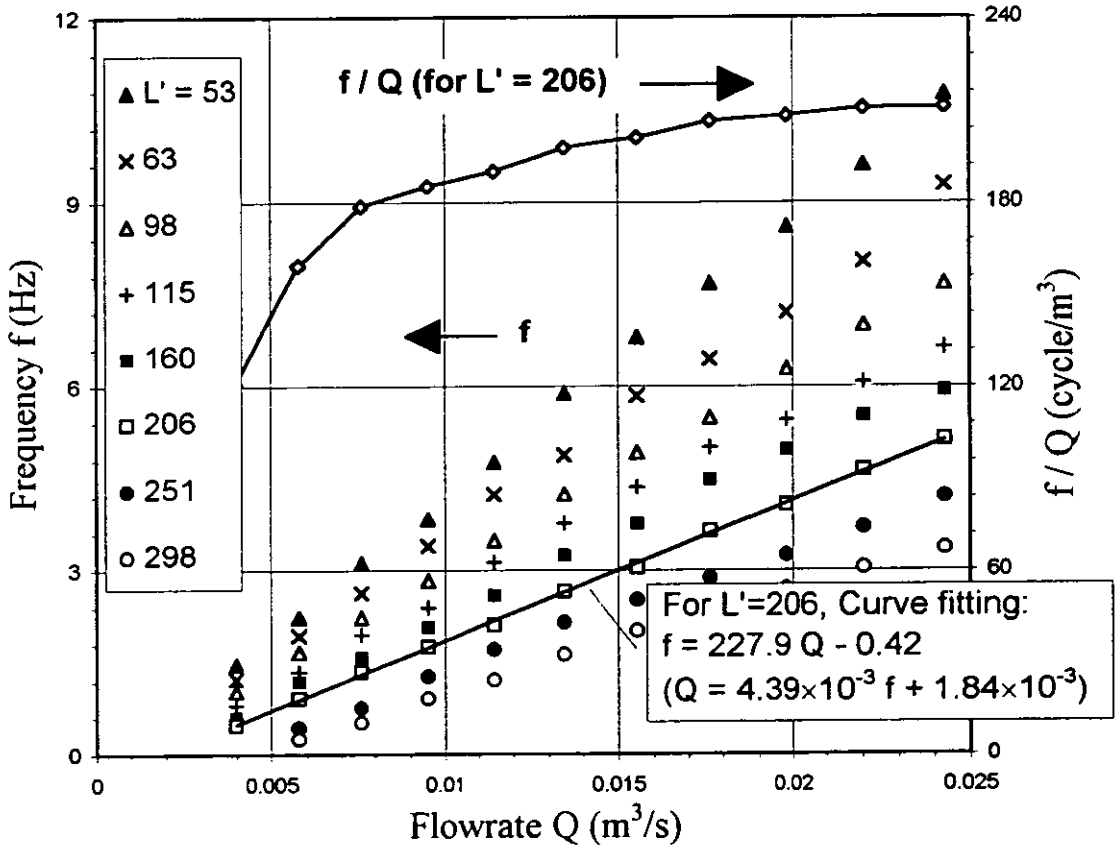

Fig. 14. CSV flowmeter optimising L' for relative pulse amplitude

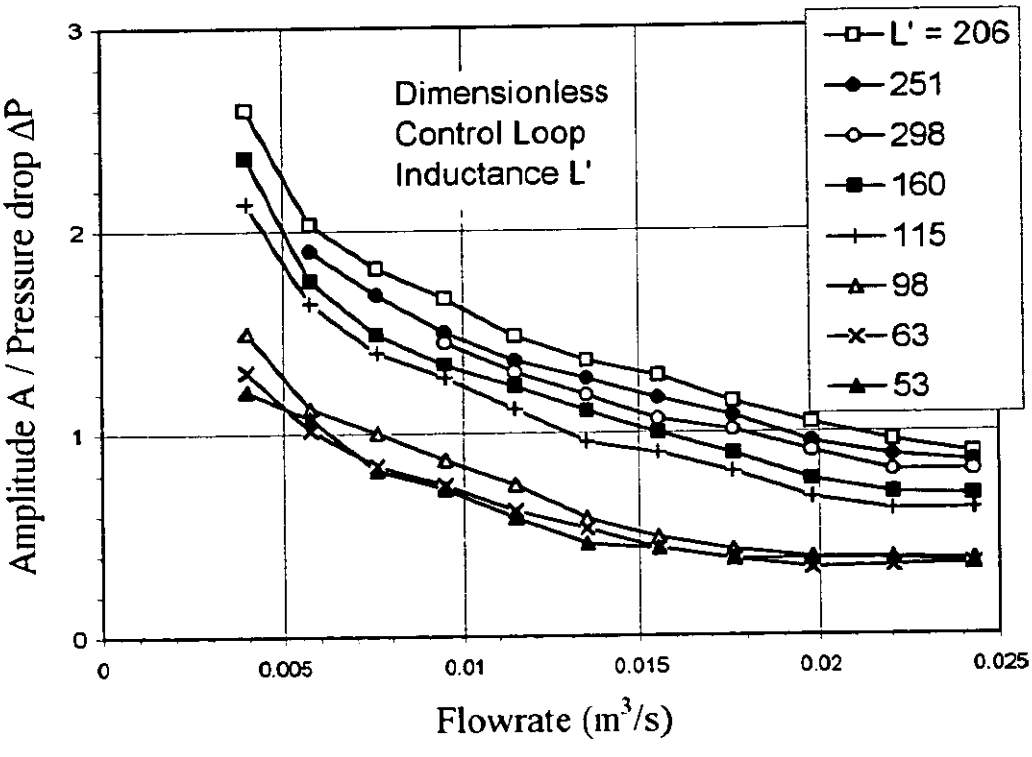

Fig.15. Mean pressure drop of CSV flowmeter

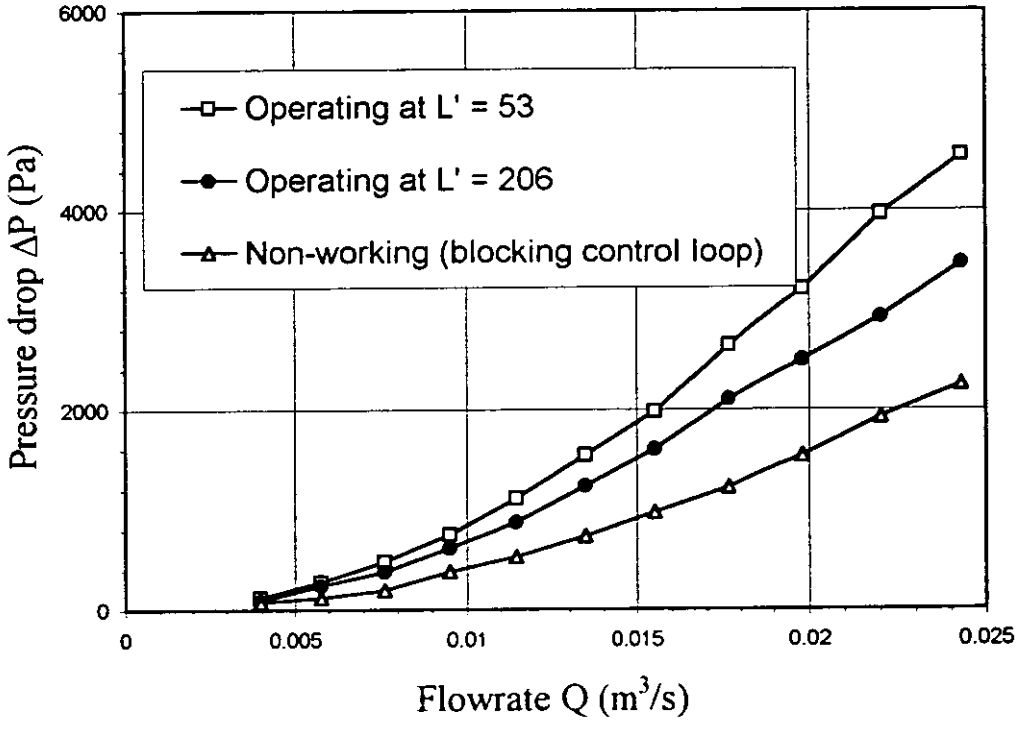

Fig. 16. Comparing the relative pulse amplitude of BV and CSV flowmeters

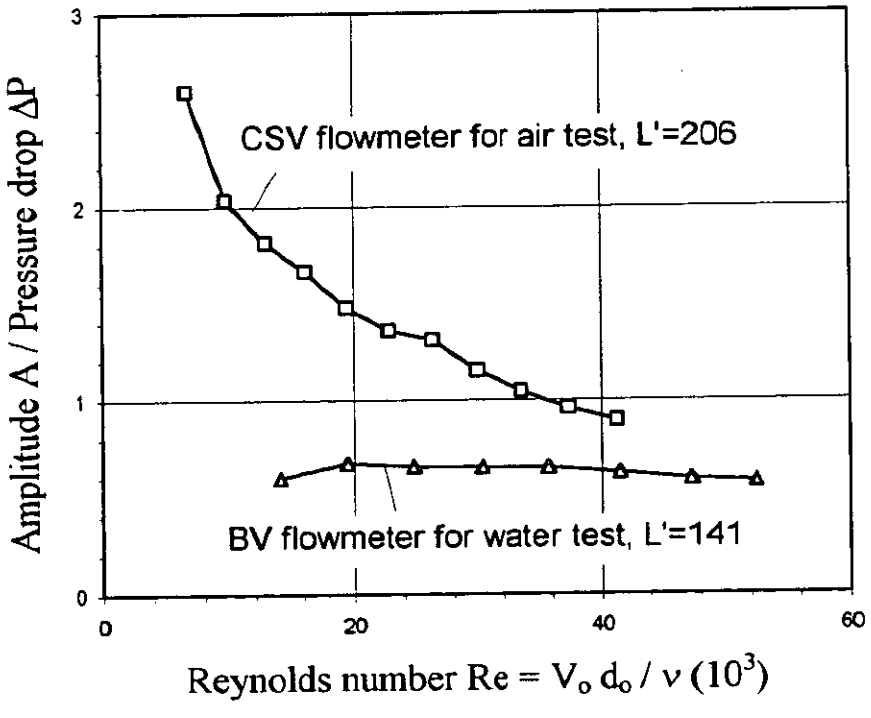

Fig.17. Overall dimensionless flowmeter calibration (refer to normalised diameter)